Available online at www.sciencedirect.com
ScienceDirect
Journal of the European Ceramic Society 31 (2011) 2267–2275
www.elsevier.com/locate/jeurceramsoc

Original article

Influence of WC particles on the microstructural and mechanical properties of 3 mol% Y_2O_3 stabilized ZrO_2 matrix composites produced by hot pressing

N. Ünal [a,b,*], F. Kern [a], M.L. Öveçoğlu [b], R. Gadow [a]

[a] Universität Stuttgart, Institut für Fertigungstechnologie Keramischer Bauteile (IFKB), Allmandring 7b, 70569 Stuttgart, Germany
[b] Particulate Materials Laboratories, Department of Metallurgical and Materials Engineering, Faculty of Chemical-Metallurgical Engineering, Istanbul Technical University, Maslak, 34469 Istanbul, Turkey

Received 29 April 2010; received in revised form 10 May 2011; accepted 22 May 2011
Available online 15 June 2011

Abstract

Yttria stabilized polycrystalline tetragonal zirconia (Y-TZP)–tungsten carbide (WC) composites were fabricated by hot pressing. Yttria (Y_2O_3) stabilizer content was kept at 3 mol% to ensure the phase structure of the Y-TZP composites to be tetragonal. To increase the moderate hardness of the 3 mol% Y_2O_3 added TZP structure, hard WC particles were added with various proportions up to 40 vol%. The TZP/WC composites were sintered at different sintering temperatures between 1450 and 1550 °C.

The mechanical and microstructural properties of the resulting composites as well as the phase compositions were investigated. Reciprocating pin-on-disk tests were carried out to determine the wear behavior of the Y-TZP/WC composites. Using bi-modal WC reinforcement, the performance of the composite against wear was improved. Using dry wear sliding conditions under 55 N normal load and 45 km sliding distance, the worn volume of the 75 vol% nanosized – WC distributed 3Y-TZP/40WC composite was about 0.003 mm^3.

Keywords: Hot pressing; Y-TZP/WC composites; Tribology; Characterization; Zirconia (ZrO_2)

1. Introduction

Structural ceramics combining high hardness, toughness, strength and wear resistance can be interesting materials for engineering applications such as cutting tools, punching and stamping dies. Zirconia (ZrO_2) is an example of such structural ceramics. Enhancement in toughness for ZrO_2 ceramics is associated with the martensitic phase transformation from metastable tetragonal phase to monoclinic phase.[1–3] This high fracture toughness value improves the wear resistance of ZrO_2 as well as its hardness.[4] However, hardness of ZrO_2 is only moderate, thus addition of hard phases such as transition metal carbides, borides or nitrides (e.g. TiN and WC) can substantially contribute to hardness increases without affecting the toughness of the ZrO_2 matrix.[5]

There are two main factors which enhance the wear performance of a composite; first is the mechanical properties of the reinforcing phase and the matrix, secondly microstructure of the composite which is influenced by particle size and distribution, volume fraction, shape of the reinforcement.[6] Monolithic ceramics generally are not able to withstand abrasive environments due to their relatively low strength and fracture toughness. However, for the ceramic matrix composites, finely and homogeneously dispersed harder particles enhance the mechanical properties of the matrix.[7] It has been shown by Jiang et al.[5] that WC enhances the hardness and wear resistance of the ZrO_2–WC nanocomposites since generally carbide additions hinder the grain growth of the matrix. Wear of composites also depends on the spacing between reinforcement particles, which can be adjusted by adding small reinforcement particles dispersed in the matrix.[6] Large reinforcing particles usually bear most of the wearing force[8,9] while uniformly dispersed small particles contribute to strengthening of the matrix.[10,11] Therefore, if a composite consists of both large and small reinforcing particles, it could have higher resistance to wear than the one reinforced by either only large particles or small particles.

* Corresponding author at: Universität Stuttgart, Institut für Fertigungstechnologie Keramischer Bauteile (IFKB), Allmandring 7b, 70569 Stuttgart, Germany. Tel.: +49 421 2246 123; fax: +49 421 2246 300.
E-mail address: nil_unal@yahoo.com (N. Ünal).

0955-2219/$ – see front matter © 2011 Elsevier Ltd. All rights reserved.
doi:10.1016/j.jeurceramsoc.2011.05.032

In this study, the effect of mechanical and microstructural properties of yttria stabilized polycrystalline tetragonal zirconia (Y-TZP)–tungsten carbide (WC) composites (Y-TZP/WC composites) on their tribological behavior was investigated. The changes in the WC dispersion amount and WC particle size distribution as well as processing conditions were characterized by X-ray diffraction (XRD), scanning electron microscopy (SEM) and with several mechanical tests.

2. Experimental procedure

Y-TZP/WC composites were prepared by homogeneously dispersing commercially available co-precipitated 3 mol% Y_2O_3 stabilized ZrO_2 powder and 0–40 vol% WC particles by attrition milling. Milling was performed in n-propanol to break the agglomerates mechanically and hence to obtain a homogenous microstructure. Milling was carried out for 1 h in a steel vial using 1 mm Ø WC/Co balls with 6:1 ball to powder ratio (BPR). As-milled powders were retrieved by drying the resulting dispersions in a rotating vacuum dryer and sieving with 35 mesh. For the preparation of the nano-WC powders, high energy Spex™ mixer mill was used in dry conditions for 10 min in a WC/Co milling system. The properties of the starting powders are listed in Table 1. Powders were hot pressed in vacuum atmosphere using a heating rate of 50 K/min under 30 MPa for 1 h in thin boron nitride coated graphite moulds. Different sintering temperatures ranging from 1450 to 1550 °C were applied to optimize mechanical properties.

Using standard metallographic procedures, the hot pressed disks were ground and polished for further tests. Archimedes method was carried out in ethanol to measure the densities of the composites. 3 point bending tests using the DIN EN ISO 6872 standard[12] was applied to five bending bars of each sample at room temperature to determine the flexural strength. Vickers hardness measurements were carried out on the hot pressed samples using a 10 kg load for 10 s. By utilizing the Niihara's equation,[13] the fracture toughness values of the composites were calculated from the crack length measurements obtained with HV_{10} indentations. Young's modulus and Vickers microhardness values were determined using a Fischerscope™ HCU microhardness test machine by applying 10 indentations under a load of 100 g for 10 s on each sample. Unlubricated reciprocating wear tests were performed using a pin-on-disc machine (Johann Fischer™ Aschaffenburg) with a 5 mm diameter WC/Co pin at ambient temperature and humidity. The balls were renewed for each experiment. The normal load and sliding speed was 55 N and 0.07 m s^{-1}, respectively. For each test, a total sliding distance of 45 km was travelled on a 5 mm stroke. Fig. 1 is a sketch representing a brief model of the reciprocating wear (friction) test which was performed on the polished surface of the composites. Friction force was monitored simultaneously using a force transducer. Surface profiles of the worn surfaces and the wear volumes were measured using a profilometer (Mahr™ Perthometer PGK).

Table 1
The characteristics of the starting powders.

Powder material	Particle size	S_{BET} (m^2/g)	Supplier	Grade
3Y-TZP	590 nm[a]	6.80[b]	Tosoh	TZ-3YS-E
WC	1.49 μm[a]	0.93[a]	Alfa Aesar	WC
Nano-WC	184 nm[a]	1.64[a]	Milled	WC

[a] Measured data.
[b] Supplier's data.

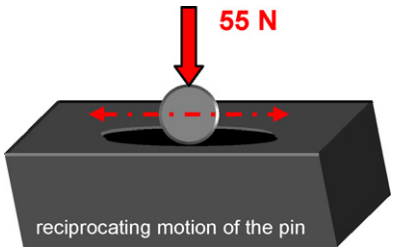

Fig. 1. The sketch of the tribological reciprocating wear test.

Microstructural investigations and observations of the wear traces were carried out using a Leo™ VP 438 scanning electron microscope (SEM) operated at 15 kV. XRD investigations of the sintered samples were carried out using a Bruker™ D-8 Advance XRD (Cu Kα radiation, λ = 0.15418 nm) diffractometer at 40 kV and 40 mA settings in the 2θ range from 25° to 80°. All XRD experiments were conducted on the polished composite surfaces.

3. Results and discussion

In our previous study, it was found out that for co-precipitated zirconia powders, 3 mol% Y_2O_3 stabilizer content was the optimum amount to achieve the highest Young's modulus, hardness, and indentation toughness values.[14] The indentation toughness value of the 2Y-TZP/WC (40 vol% WC) composite was 5.20 MPa $m^{1/2}$ which was increased to 6.54 MPa $m^{1/2}$ for the 3Y-TZP/WC (40 vol% WC) composites; both fabricated using the same parameters.[14] Further, the 3 mol% Y_2O_3 stabilized the tetragonal ZrO_2 phase at room temperature and improved the toughness.[14] The Vickers hardness and indentation toughness results of the 3Y-TZP/WC (32 vol% WC) composites with respect to sintering temperatures are shown in Fig. 2. Hereafter, 3Y-TZP/WC composite having 40 vol% WC phase will be named as 3Y-TZP/40WC and the other compositions will be named similarly as well.

In order to optimize the sintering temperature, samples were hot pressed at several temperatures between 1450 °C and 1550 °C. In contrast to hardness and density enhancement, indentation toughness values declined sharply with increasing sintering temperatures. Furthermore, the flexural strength value decreased slightly from 1179 MPa to 990 MPa as sintering temperature increased from 1450 °C to 1550 °C. Samples were fully densified ($\rho > 98\%$ relative) even at 1450 °C, therefore this sintering temperature was chosen for the rest of the experiments.

Detailed information about the grain size of the WC dispersion phase was obtained by back scattered electron (BSE) images given in Fig. 3. Fig. 3a and b are the BSE images taken from the crack path of 3Y-TZP/32WC composites sintered at 1450 °C

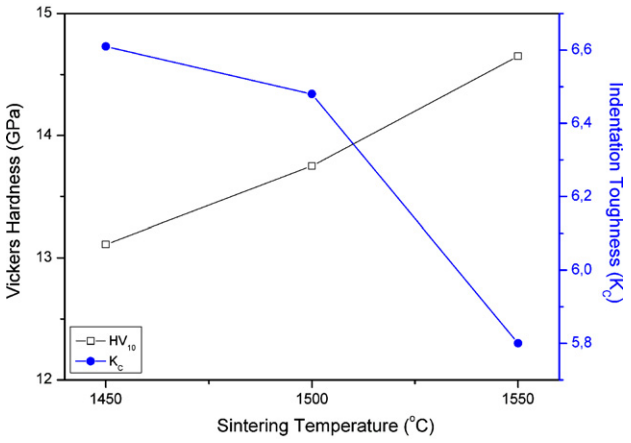

Fig. 2. The mechanical properties of the 3Y-TZP/32WC composite with respect to sintering temperature.[14].

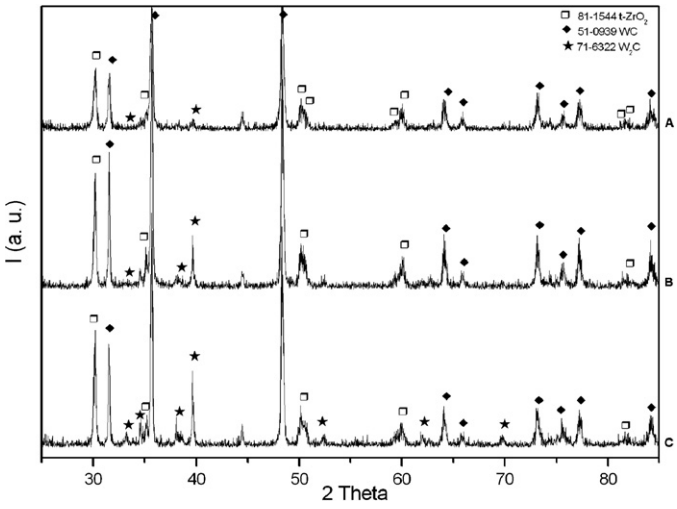

Fig. 4. XRD patterns of the 3Y-TZP/32WC composites hot pressed at 1450 °C, 1500 °C, and 1550 °C.

and at 1500 °C, respectively. On top of each image, there is a 5k× magnified version of the non-cracked surface. The light grey phases indicate the WC phases and the Y-TZP matrix was determined as the dark grey phase.

It is commonly believed that fracture toughness increases with decreasing grain size as composition and other microstructural variables are held constant.[15–17] For transformation toughened composite materials, this is only partially true as the increasing size of zirconia grains leads to increase in transformability and increasing fracture toughness owing to an increasing transformation zone size.[18,19] However, this effect should not be overstressed as grains exceeding a critical threshold size will transform to monoclinic during cooling with a significant decrease in tetragonal content and thus cause toughness decreases.[19] According to BSE images in Fig. 3, with increasing sintering temperature, WC grain growth was not observed. On the other hand, the sizes of ZrO_2 grains could not be precisely measured since the grain boundaries were not distinctly etched using both thermal and chemical etching. Nevertheless, the study of Singh et al.[20] pointed out that, as the sintering temperature increased from 1450 °C to 1550 °C, the grain size of pure co-precipitated 3Y-TZP ceramic increased slightly from 400 nm to 700 nm. However, the fracture toughness values remained constant at around 5 MPa $m^{1/2}$. Our previous study[14] revealed that as the sintering temperature increased from 1450 °C to 1550 °C, the indentation toughness of the 3Y-TZP/32WC composite decreased slightly although density, hardness and Young's modulus values were improved. Therefore, it is expected that at higher temperatures, larger grains tend to transform to monoclinic phase during cooling which lowered the toughness.

The XRD patterns of the 3Y-TZP/32WC composites sintered at 1450 °C, 1500 °C, and 1550 °C are given in Fig. 4A–C, respectively. Three major peaks in all figures matched the ICDD card values of the stable ZrO_2 phase (Bravais lattice: primitive tetragonal, Space Group: $P42/nmc$),[21] the WC phase (Bravais lattice: primitive hexagonal, Space Group: $P\bar{6}m2$)[22] and the W_2C phase (Bravais lattice: primitive hexagonal, Space Group: $P6_3/mmc$).[23] The W_2C phase emerges in the microstructure at 1450 °C and its amount continuously increases with increasing sintering temperatures (traces B and C of Fig. 4). The peak which is around 45° could not be identified. Since this peak was observed in all XRD scans, it is believed that it was reflected from the base-holder.

According to XRD results presented in Fig. 4, the reduction of the indentation toughness at higher sintering tempera-

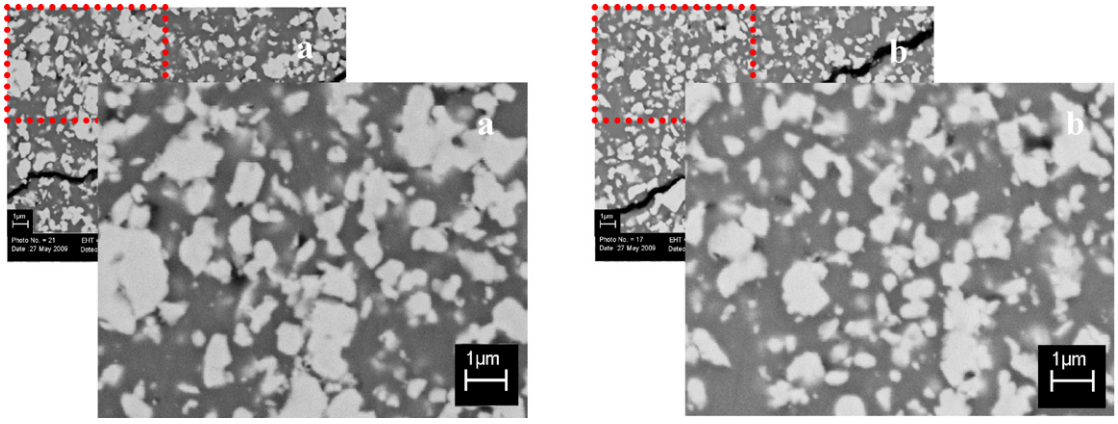

Fig. 3. Back-scattered electron (BSE) images of the 3Y-TZP/32WC composites sintered at: (a) 1450 °C and (b) 1500 °C. From a selected part of the 5k× BSE images, equally magnification applied to create the top detailed images, WC (white phase), 3Y-TZP matrix (grey phase).

tures can most probably be attributed to increasing amount of ditungsten carbide (W_2C) phase. Zirconia (ZrO_2) seems to react with tungsten carbide (WC) forming ditungsten carbide (W_2C) and carbon monoxide (CO) due to the equation: $ZrO_2 + 6WC \rightarrow 3W_2C + 2CO + ZrC$.[24] On the basis of XRD measurements, Haberko et al.[24] reported the formation of the ZrC phase in the 20 vol% WC dispersed ZrO_2 matrix composites sintered at 1700 °C. Moreover, they also identified the ZrC phase in TEM investigations of the samples sintered around 1400 °C. It is supposed that ZrO_2 incorporated some carbide either into the anionic sublattice or as nanoscale zirconium carbide making the reaction product very difficult to be detected in the XRD patterns. Anionic lattice stabilization by carbon or nitrogen can stabilize tetragonal phase and lower transformability. W_2C phase is equally hard but more brittle than WC and may contribute to the loss of toughness at higher sintering temperatures.[25]

The effect of WC amount on the mechanical and microstructural properties of the fine 3Y-TZP matrix composites was observed by reinforcing with 5–40 vol% micron-sized WC particles. The most significant influence of WC addition was the increase of the indentation toughness while hardness remained similar. The carbide reinforcements hinder densification of the composites with increasing WC addition.

The mechanical and physical properties of the 3Y-TZP matrix composites containing different WC contents are given in Table 2. Following sintering at 1450 °C, 3Y-TZP matrix composite samples were ground and polished. As can be seen in Table 2, relative density % values decrease with increasing WC content, inferring that WC inclusions restrain the densification. Nevertheless, except for the sample containing 40 vol% WC, the density values of all sintered samples (3Y-TZP and 3Y-TZP/WC composites) were fairly good. The flexural strength values fluctuated with increasing WC contents, but the 40 vol% WC containing composite displayed the lowest strength value. This composite also had the lowest density value as a result of incomplete sintering. Regarding the indentation toughness measurements, no evidence was found whether the cracking mode was palmqvist or median. However, Niihara's palmqvist crack equation[13] is more suitable to our case as crack to indent ratio size (c/a) is low. For all samples, indentation toughness and hardness values increased systematically with increasing WC content.

The thermal expansion mismatch between the 3Y-TZP matrix and WC particles was probably caused by residual thermal stresses within and around WC particles during furnace cooling to room temperature. The thermal expansion value of the 3Y-TZP matrix (α_m) is $11.0 \times 10^{-6}\ K^{-1}$ [26] and the WC particle (α_p) is $5.2 \times 10^{-6}\ K^{-1}$, i.e. $\alpha_m > \alpha_p$.[26] Subsequent to cooling, the interface was left under compressive load. Depending on the strength of the interface, tangential tensile stresses could cause radial microcracks around the WC particles in the ZrO_2 matrix associated with transformation around WC grains. On the other hand, during cooling this would lower the toughness.[26–28] A weak interface will facilitate crack deflection which would improve toughness.

Lange[29] has pointed out that the incorporation of a second phase with high modulus increases toughness significantly. Thus, the high Young's modulus of WC (700 GPa) will contribute strongly to toughness of the composites. Increase in toughness values with WC content indicates that mechanisms hindering crack propagation were dominant.[10] On the basis of Table 2, the 3Y-TZP composite containing 32 vol% WC has the best overall mechanical properties.

Fig. 5a–c are the SEM micrographs taken from the 3Y-TZP matrix reinforced with 20 vol%, 32 vol% and 40 vol% WC particles, respectively. Due to the activation of the crack deflection, crack branching and bridging mechanisms observed on the etched crack surfaces shown in Fig. 5, toughness increased.

Table 2
Mechanical properties of the 3Y-TZP/WC composites hot pressed at 1450 °C.

WC (vol%)	Relative density (%)	Strength (MPa)	E (GPa)	HV_{10} (GPa)	K_C, PQ (MPa $m^{1/2}$)	K_C, MED (MPa $m^{1/2}$)
40	95.26	452	312 ± 14	13.80 ± 0.50	6.54 ± 0.20	8.52 ± 0.39
32	98.34	1179	312 ± 5	13.11 ± 0.29	6.52 ± 0.21	8.56 ± 0.41
20	98.87	969	273 ± 3	13.60 ± 0.45	6.48 ± 0.28	8.64 ± 0.58
10	99.20	1476	272 ± 2	12.85 ± 0.38	5.67 ± 0.11	7.13 ± 0.25
5	99.60	1282	265 ± 2	14.22 ± 0.04	5.22 ± 0.08	6.11 ± 0.17
0	100.00	1291	235 ± 3	14.24 ± 0.18	5.05 ± 0.03	5.97 ± 0.06

Toughness measurements were calculated by Niihara palmqvist (PQ) and median (MED) equation.

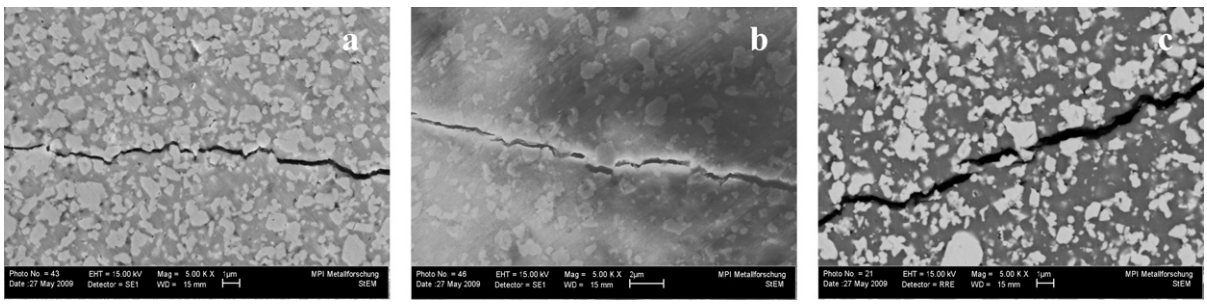

Fig. 5. Propagation of an indentation crack on the 3Y-TZP matrix containing: (a) 20 vol% WC, (b) 32 vol% WC and (c) 40 vol% WC.

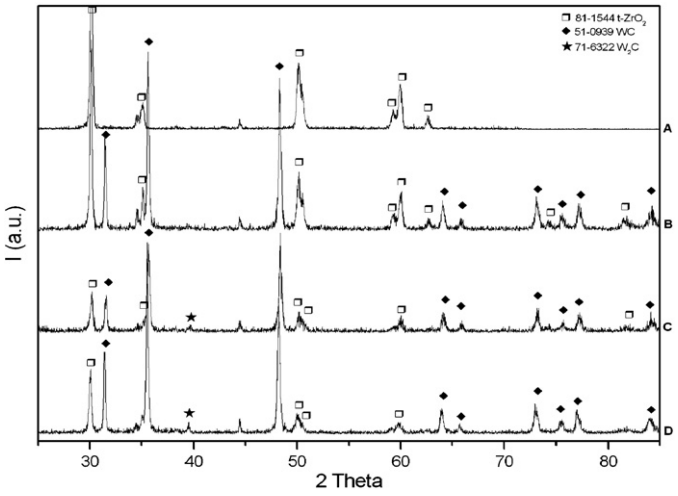

Fig. 6. XRD patterns of the 3Y-TZP/WC composites hot pressed at 1450 °C reinforced with: (A) 0 vol%, (B) 20 vol%, (C) 32 vol% and (D) 40 vol% WC particles.

Fig. 6 shows XRD patterns taken from the 3Y-TZP/WC composites hot pressed at 1450 °C reinforced with: (A) 0 vol% WC, (B) 20 vol% WC, (C) 32 vol% WC and (D) 40 vol% WC particles. As seen in Fig. 6, with increasing WC content in the 3Y-TZP matrix, more W_2C phase was formed. It is believed that zirconia powders formed a gas tight matrix at lower sintering temperatures and prevented the escape of gaseous products like CO which eventually enabled the formation W_2C. This concept was followed by Jiang et al.[5] successfully using the more silica rich and sinterable Daichi HSY-3U zirconia powder.

Fig. 7 shows in situ high temperature XRD patterns of the 3Y-TZP/40WC composite taken between room temperature and 1450 °C at temperature increments of 50 °C. These in situ XRD patterns during heating up from RT to 1300 °C indicated that in addition to some unidentifiable peaks occurring at very low 2θ angles, no evidences of any phase changes were observed. As expected, less than 20°, monoclinic ZrO_2 had a peak with a low intensity which is marked in Fig. 7b. According to the analyses, this phase started to form at temperatures above 1000 °C.

Thus, on the basis of the presented data, increasing the sintering temperature in order to obtain higher density and better mechanical properties seems an invalid strategy. Based on existing literature the assignment of toughness reduction to a single cause seems incorrect. The effect is probably caused by a superposition of several phenomena. However, it can be assumed that the main reason for high indentation toughness results in general are due to the combination of martensitic phase transformation with crack deflection, crack branching and bridging mechanisms.

The effect of WC amount on wear performance was examined via unlubricated sliding pin-on-disc tests. The volumetric wear rate (kv) was calculated by using Archard's equation[30] given in Eq. (1):

$$kv = \frac{V_{\text{wear}}}{F_{\text{N}} \times s} \left(\frac{\text{mm}^3}{\text{N m}} \right) \quad (1)$$

where F_{N} is the normal load, s the sliding distance, V_{wear} is the wear volume and kv is the wear rate. Wear test results of 3Y-TZP/WC composites hot pressed at 1450 °C are listed in Table 3.

Table 3
Dry reciprocating wear test results of 3Y-TZP/WC composites under 55 N normal load with a sliding distance (s) of 45 km against WC–Co.

WC (vol%)	Friction force (N)	Friction coefficient (μ)	Wear volume (mm^3)	kv (10^{-8} $\text{mm}^3/\text{N m}^{-1}$)
40	21.31	0.39	0.02	0.80
32	22.92	0.42	0.03	1.21
20	26.58	0.48	0.04	1.62
0	37.40	0.68	0.15	6.06

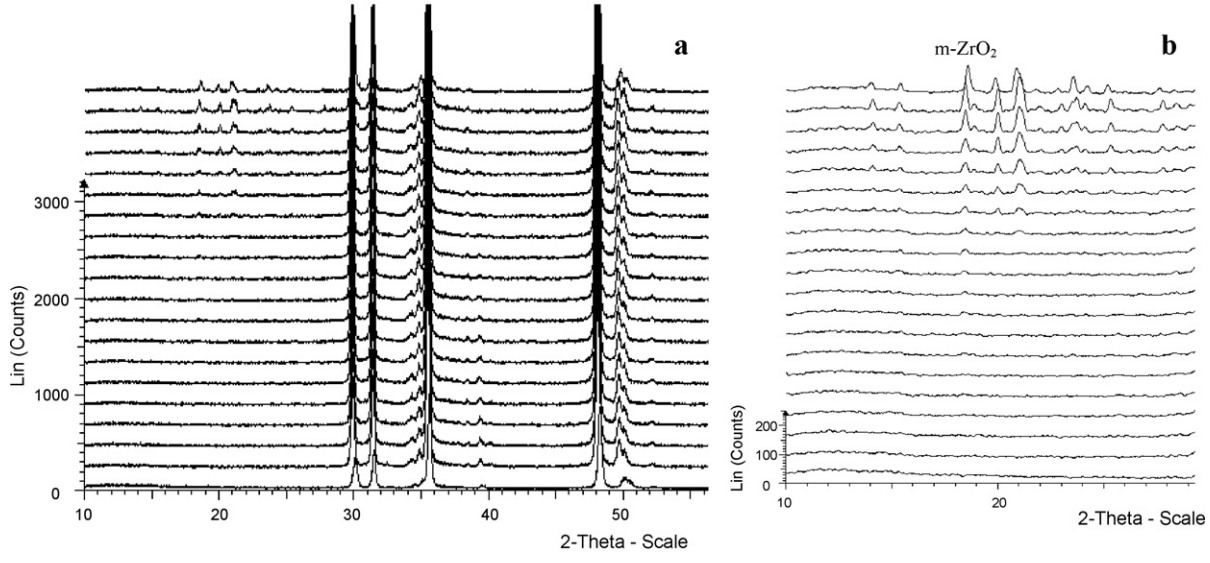

Fig. 7. In-situ XRD patterns of 3Y-TZP/40WC composite starting from ambient temperature up to 1450 °C with 50 °C increment (a), detailed view up to $2\theta = 30°$ (b).

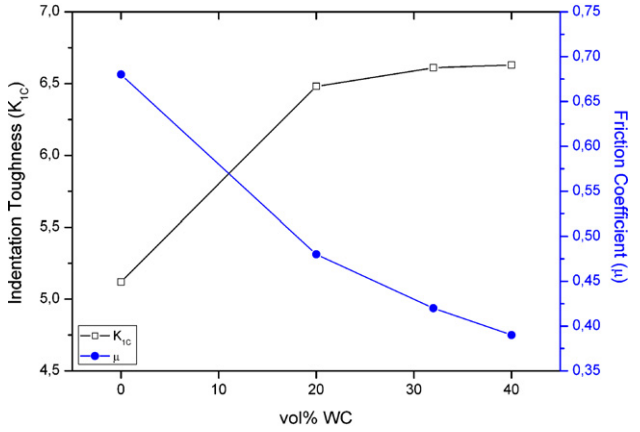

Fig. 8. Indentation toughness (K_C) and friction coefficient (μ) values of the ZrO_2/WC composites with respect to WC vol% amount.

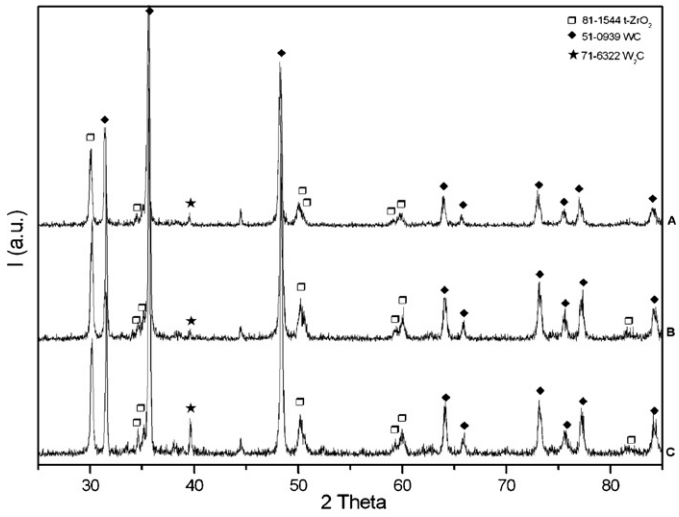

Fig. 9. XRD patterns of the bimodal particle size distributed 3Y-TZP/40WC composites. Coarse WC particle dispersion value of 100 vol% (A), 75 vol% (B) and 25 vol% (C), respectively.

As clearly seen in Table 3, the presence of homogeneously dispersed hard WC particles added in increasing amounts significantly enhanced the tribological behavior of 3Y-TZP matrix composites. The worn volume was reduced nearly 15% with 40 vol% WC addition. Although the hardness, strength, and density of 3Y-TZP/40WC were lower than the pure 3Y-TZP matrix, the improvement in wear resistance could be attributed to the high indentation toughness because the critical load of crack propagation was influenced by toughness. Bhushan[31] stated that low toughness reduces wear resistance by introduction of microfracture at contact surfaces in sliding.

Fracture toughness (K_{1C}) and friction coefficient (μ) values of the ZrO2/WC composites with respect to WC amount are presented in Fig. 8. As the toughness increases with increasing WC amounts, the friction coefficient decreases, implying that the wear resistance increases. In the present study, it may be speculated that higher contents of WC will increase the thermal conductivity and thus the long term stability of the zirconia by preventing heating up. The fact that the worn surfaces did not show any evidence of spallation or cracking support this assumption that the matrix remained stable during the wear test and was able to keep hold of the dispersed WC.

3.1. Effect of bimodal WC particle size distribution

In order to enhance the mechanical properties of the compacts further, different percentages of nano-WC particles were mixed with micron-sized WC particles. Packing density of the bi-modal composites was increased by increasing particle size distribution broadening. In addition to improved sintered density, higher Young's modulus and indentation toughness was achieved. In Table 4, relative densities and some mechanical properties of the 3Y-TZP/WC (40 vol%) composite as a function of the vol% coarse WC are listed.

The reason for the slight increase in the hardness and enhancement in the indentation toughness of the 75 vol% coarse WC dispersed 3Y-TZP/40WC composite can be explained by XRD phase analysis. According to Fig. 9, it is clear that W_2C phase formation was increased with higher nano-WC addition. Brittle W_2C enhanced hardness but indentation toughness was decreased slightly when nano-WC increased to 75 vol%.

In addition to improvements in indentation toughness and strength, wear resistance of the composites were enhanced significantly by nano-WC additions. As indicated in Table 5, the wear rate was decreased from 0.8×10^{-8} to 0.12×10^{-8} $mm^3/N\,m^{-1}$. Even with dry sliding conditions under relatively high normal load and long operation conditions the worn volume was 0.003 mm^3 for the 25% coarse nano-WC

Table 5
Dry reciprocating wear test results of 3Y-TZP/40WC composites as a function of coarse-WC content under 55 N normal load with a sliding distance (s) of 45 km.

Coarse WC (vol%)	Friction force (N)	Friction coefficient (μ)	Wear volume (mm^3)	kv (10^{-8} mm^3 /N m^{-1})
100	21.31	0.39	0.02	0.80
75	20.36	0.37	0.01	0.40
25	19.38	0.36	0.003	0.12

Table 4
Relative density % values and mechanical properties of 3Y-TZP/40WC composites sintered at 1450 °C as a function of coarse-WC content.

Coarse WC (vol%)	Relative density (%)	Strength (MPa)	E (GPa)	HV_{10} (GPa)	K_C, PQ (MPa $m^{1/2}$)	K_C, MED (MPa $m^{1/2}$)
100	95.26	452	312 ± 14	13.80 ± 0.50	6.54 ± 0.20	8.52 ± 0.39
75	97.00	763	367 ± 4	13.82 ± 1.05	6.84 ± 0.64	8.89 ± 1.31
25	98.01	827	371 ± 3	15.92 ± 0.30	6.85 ± 0.35	8.56 ± 0.68

Toughness measurements were calculated by Niihara palmqvist (PQ) and median (MED) equation.

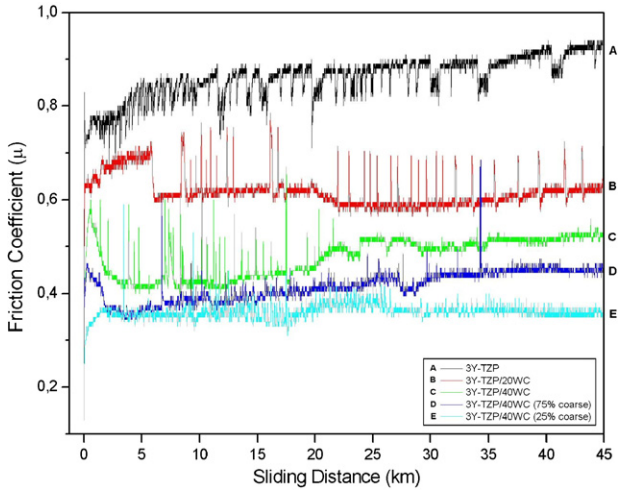

Fig. 10. Friction coefficient curves of the 3Y-TZP composites hot pressed at 1450 °C as a function of sliding distance under 55 N constant normal load with a sliding velocity of 0.07 m s^{-1}: (A) 3Y-TZP composites without WC addition and containing, (B) 20 vol% WC, (C) 40 vol% WC, (D) 40 vol% WC (75% coarse + 25 vol% nano-sized) and (E) 40 vol% WC (25% coarse + 75 vol% nano-sized).

distributed 3Y-TZP/40WC composite. The wear resistance was enhanced significantly and the value is satisfactory compared to those reported in the literature.[32,33]

Coefficient of friction (COF) was recorded simultaneously by the computer and the values are shown in Fig. 10. Fig. 10A–E present the coefficient of friction values (μ) versus sliding distance (in km) of the 3Y-TZP composites hot pressed at 1450 °C. In Fig. 10, the lines represent the samples by order of without WC addition (Fig. 10A) and containing 20 vol% WC (Fig. 10B), 40 vol% WC (Fig. 10C), 40 vol% WC (75% coarse + 25 vol% nano-sized) (Fig. 10D) and 40 vol% WC (25% coarse + 75 vol% nano-sized) (Fig. 10E). For a constant normal load, the friction force fluctuated with respect to sliding distance. However, the fluctuations were very small in the 25% coarse WC dispersed 3Y-TZP/40WC composites. In general, the COF curve of the pure 3Y-TZP material has a shape different oscillation; it was just decreased from the constant COF value. This behavior can occur due to hard on soft WC–Co/ZrO_2 sliding contact which cause adhesion. On the other hand, with hard WC additions to the matrix, hard on hard WC–Co/WC sliding increased the friction coefficient. Steady state regime was obtained after about 35 km sliding distance of the all range particle size distributed 3Y-TZP/40WC composites. The friction coefficient levels decrease with increasing WC content. Best and most constant values were obtained with 40 vol% WC (25% coarse).

The inverted profiles of the abraded surfaces are given in Fig. 11. By means of the 3D surface topographies, it is clear that the 3Y-TZP matrix structure without WC reinforcement had a deeper wear track then the ones with WC additions. Relatively flat and shallow abraded surface of 3Y-TZP/40WC (25% coarse) was obtained with bi-model particle size WC-reinforcement. Consequently, these large and small WC reinforcing particles enhanced the wear resistance considerably more than those containing only large or small WC particles.

Fig. 12a–c are respective SEM micrographs taken from the middle part of the wear traces of the 3Y-TZP matrix composites without WC addition and those containing 40 vol% WC, and 40 vol% WC (25% coarse + 75 vol% nano-sized) at a total sliding distance of 45 km under a normal load of 55 N.

The SEM images of Fig. 12 reveal that on the wear layer there was neither an adhesion of the debris nor any microcracks along the wear trace. Initially, all the abraded material was removed from the debris layer and did not stick onto the wear layer afterwards. The same wear behavior was found in all composites. The bimodal particle size distribution did not have any effect on the surface morphology of the worn surface.

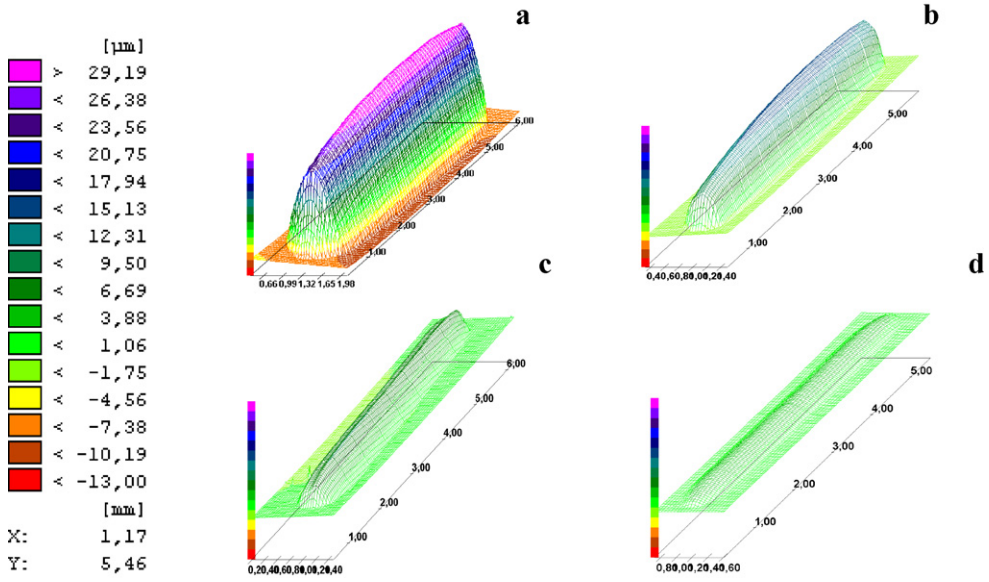

Fig. 11. Inverted 3D surface profiles of the parts after 45 km unlubricated wear test run. The tracks belong to (a) 3Y-TZP, (b) 3Y-TZP/20WC, (c) 3Y-TZP/40WC and (d) 3Y-TZP/40WC (25% coarse), respectively.

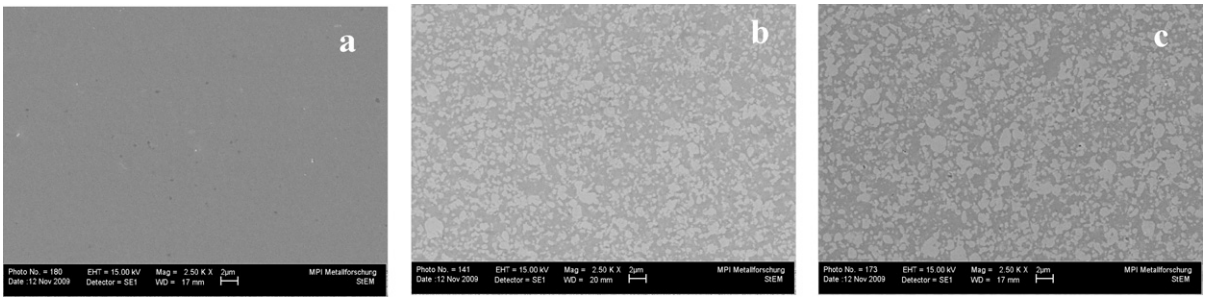

Fig. 12. SEM images taken from the middle part of the wear traces of ZrO_2/WC composites after 45 km run, (a) 3Y-TZP, (b) 3Y-TZP/40WC and (c) 3Y-TZP/40WC (25% coarse), respectively.

4. Conclusions

Based on the results reported in the present investigation, the following conclusions can be drawn:

1. WC addition to the 3 mol% Y_2O_3 stabilized ZrO_2 matrix enhanced the indentation toughness values while hardness values remained constant. The 3Y-TZP reinforced with 32 vol% WC has the overall best mechanical and microstructural properties, i.e. the highest strength, Young's modulus and indentation toughness. WC reinforcements higher than 32 vol% WC resulted in the decline of the relative density values.
2. The main reason for the enhancement of indentation toughness with increasing WC content can be attributed to crack deflection, crack branching and bridging mechanisms incorporation with phase transformation toughening. Additionally, homogeneously distributed WC which has high modulus increased toughness significantly.
3. The optimized sintering temperature for the Y-TZP/WC composites was determined as 1450 °C. Higher temperatures led to a decline in flexural strength and indentation toughness due to increasing amount of the W_2C phase identified in the XRD patterns.
4. The tribological behavior of the 3Y-TZP matrix was enhanced significantly by the presence of homogeneously dispersed hard WC particles. The worn volume was reduced nearly 15% with 40 vol% WC addition. In addition, bimodal WC particle size distribution of nano-sized WC and coarse WC particles improved the relative density, Young's modulus, and indentation toughness considerably. Besides enhanced mechanical properties, superior wear resistance was obtained by nano-WC additions. Even with dry sliding conditions under relatively high normal load and long operation conditions, the worn volume was 0.003 mm^3 for the 75 vol% nano-sized WC distributed 3Y-TZP/40WC composite.

Acknowledgement

This research was made possible by a research grant provided by Deutscher Akademischer Austausch Dienst (DAAD) and this is gratefully acknowledged.

References

1. Rühle M, Evans AG. High toughness ceramics and ceramic composites. *Prog Mater Sci* 1989;**33**:85–167.
2. Evans AG. Perspective on the development of high-toughness ceramics. *J Am Ceram Soc* 1990;**73**(2):187–206.
3. Lange FF. Transformation-toughened ZrO_2: correlations between grain size control and composition in the system ZrO_2–Y_2O_3. *J Am Ceram Soc* 1986;**69**(3):240–2.
4. Fischer TE, Anderson MP, Jahanmir S. Influence of fracture toughness on the wear resistance of yttria-doped zirconium oxide. *J Am Ceram Soc* 1989;**72**(2):252–7.
5. Jiang D, Van der Biest O, Vleugels J. ZrO_2–WC nanocomposites with superior properties. *J Eur Ceram Soc* 2007;**27**:1247–51.
6. Hua J, Li DY, Llewellyn R. Computational investigation of microstructural effects on abrasive wear of composite materials. *Wear* 2005;**259**:6–17.
7. National Materials Advisory Board. *Tribology of ceramics*. USA: National Academy Press; 1988.
8. Das S, Mondal DP, Dixit G. Correlation of abrasive wear with microstructure and mechanical properties of pressure die-case aluminum hard-particle composite. *Metall Mater Trans A* 2001;**32A**:633–42.
9. Yilmaz O, Turhan H. Effect of size and volume fraction of particulates on the sliding wear resistance of CuSn composites. *Wear* 2002;**249**:901–13.
10. Zum Gahr KH. How microstructure affects abrasive wear resistance. *Metal Prog* 1979;**116**(4):46–52.
11. Kim H-M, Kim T-S, Suryanarayana C, Chun B-S. Microstructure and wear characteristics of rapidly solidified Al–Pb–Cu alloys. *Mater Sci Eng A* 2000;**287**:59–65.
12. DIN EN ISO 6872. *Dental ceramic*. Berlin: International Organization for Standardization; 1998.
13. Niihara K. A fracture mechanics analysis of indentation-induced Palmqvist crack in ceramics. *J Mater Sci Lett* 1993;**2**:221–3.
14. Ünal N, Kern F, Gadow R. Properties of zirconia–tungsten carbide composites produced by hot pressing. In: *EURO PM2009 proceedings, vol. 3*. 2009. p. 47–53.
15. Calister W. *Material science and engineering: an introduction*. 3rd edition John Wiley & Sons, Inc.; 1994. p. 193–5.
16. Dowling NE. *Mechanical behavior of materials: engineering methods for deformation, fracture, and fatigue*. Prentice Hall; 1993. p. 302–10.
17. Reed-Hill RE, Abbaschian R. *Physical metallurgy principles*. 3rd edition PWS Publishing Company; 1994. p. 737–8.
18. Swain MV. Grain size dependence of toughness and transformability of 2 mol-% Y-TZP ceramics. *J Mater Sci Lett* 1986;**5**:1159–62.
19. Ruiz L, Readey MJ. Effect of heat treatment on grain size, phase assemblage, and mechanical properties of 3 mol% Y-TZP. *J Am Ceram Soc* 1996;**79**(9):2331–40.
20. Singh R, Gill C, Lawson S, Dransfield GP. Sintering, microstructure and mechanical properties of commercial Y-TZPs. *J Mater Sci* 1996;**31**:6055–62.
21. Powder Diffraction Files. *Card No. 81-1544*. Database edition. International Centre for Diffaction Data (ICDD). Newton Square, PA 19073-3273, USA; 2006.

22. Powder Diffraction Files. *Card No. 51-0939*. Database edition. International Centre for Diffaction Data (ICDD). Newton Square, PA 19073-3273, USA; 2006.
23. Powder Diffraction Files. *Card No. 71-6322*. Database edition. International Centre for Diffaction Data (ICDD). Newton Square, PA 19073-3273, USA; 2006.
24. Haberko K, Pedzich Z, Faryna M, Dutkiewicz J, Kowal A. In: Tomsia AP, Glaeser AM, editors. *Ceramics Microstructure: Control at the Atomic Level*. New York, NY: Plenum Press; 1998.
25. Weimer AW. *Carbide, nitride and boride materials synthesis and processing*. London: Chapman & Hall; 1997.
26. Pedzich Z, Faryna M, Haberko K. In: Adali S, Verijenko E, editors. *Composite science and technology*. Durban, South Africa: University of Natal; 1996. p. 379–84.
27. Pedzich Z, Haberko K. Toughening mechanisms in the TZP–WC particulate composites. *Key Eng Mater* 1997;**132–136**:2076–9.
28. Zhan G, Lai TR, Shi JL, Yen TS, Zhou Y, Zhang YZ. *J Mater Sci* 1996;**31**:2903–7.
29. Lange FF. Transformation toughening. *J Mater Sci* 1982;**17**:240–6.
30. Archard JF, Hirst W. The wear of metals under unlubricated conditions. *Math Phys Sci* 1956;**236**(1206):397–410.
31. Bhushan B. *Modern tribology handbook*. vol. 1. CRC Press, Boca Raton, Florida; 2000.
32. Bonny K, De Bets P, Vleugels J, Silehi A, Van der Biest O, Lauwers B, et al. Sliding wear of electrically conductive ZrO_2–WC composites against WC–Co cemented carbide. *Tribol Lett* 2008;**30**:191–8.
33. Haberko K, Pedzich Z, Rog G, Bucko M, Faryna M. The TZP matrix—WC particulate composites. *J Solid State Inorg Chem* 1995;**32**:593–601.